

# Dynamic Numerical Model for a Geothermal Well

Francesco Calise<sup>a</sup>, Francesco Liberato Cappiello<sup>b</sup>, Luca Cimmino<sup>c</sup> and Maria Vicidomini<sup>d</sup>  
*DII, University of Naples Federico II, P.le Tecchio, 80, 80125 Naples, Italy*

**Keywords:** Geothermal Well, Downhole Heat Exchanger, Renewable Source of Energy, Dynamic Model.

**Abstract:** The paper proposed a detailed mathematical model that uses the TRNSYS environment to dynamically assess the thermodynamic performance of a geothermal well. This research aims to provide a fast and reliable dynamic mathematical model able to mimic the real-time operation of a geothermal well, given the depth of the well and the temperature of the surrounding soil. In addition, this model can simulate the energy performance of the downhole heat exchangers installed into the geothermal well. The results of the model indicate that the proposed model can accurately assess and simulate the performance of the geothermal well also including the energy performance of the downhole heat exchangers. In addition, this model may be exploited for dimensioning proper control strategies able to manage the temperature of the downhole heat exchanger.

## 1 INTRODUCTION

The growing concerns due to the impacts of climate change on the worldwide communities (Tapia, 2017) is increasing the interest in renewable energy sources (Calise, 2022). Geothermal energy source is constant, predictable, and reliable (Glassley, 2014, McClean and Pedersen, 2023). In addition, it is unaffected by significant seasonal variations, which dramatically affect other renewable energy sources, such as solar and wind (Glassley, 2014, McClean and Pedersen, 2023). The main issue with geothermal energy is related to the excessive costs of drilling and the complexity of the plants (Stefánsson, 2002). In this framework the development of a proper simulation model able to mimic the dynamic performance of a geothermal plant is crucial, for assessing the feasibility (Calise, 2020). Thus, the mathematical modelling of the geothermal well performance is useful for accurately describing the energy performance of geothermal plants (Buonomano, 2015). Several numerical models were developed for assessing the thermal performance of geothermal wells including downhole heat exchangers. In this framework, Ref. (Yuan, 2023) modelled vertical and

inclined wellbore to assess the profitability of advanced geothermal systems. The authors developed a 3-D model using the COMSOL software. The results provided by such model are validated against experimental measurements. The proposed model resulted reliable in evaluating the thermal energy performance of a closed-loop geothermal technology-based plants. Ref. (Yuan, 2023) proposed a 3-D mathematical model of a deep borehole heat exchanger (DBHE), developed in MATLAB environment. The main assumptions of such model are that: i) the underground thermal reservoir is isotropic and homogeneous; ii) the underground thermal reservoir physical parameters are constant over the times; iii) the heat transfer along the axis of the heat exchanger is negligible; iv) no contact thermal resistance between the pipe of DBHE and the thermal reservoir; v) the soil temperature is constant over the time. The results of such model are validated against experimental data. In conclusion, this work assessed that for the selected boundary conditions the heat transfer rate per unit of buried depth is equal to 21.99 W/m with a heat exchanger water flow rate of 60 m<sup>3</sup>/h. Ref. (Dalala, 2022) proposed a novel 1-D multi-segment model able to simulate the deep and

<sup>a</sup>  <https://orcid.org/0000-0002-5315-7592>

<sup>b</sup>  <https://orcid.org/0000-0001-6292-686X>

<sup>c</sup>  <https://orcid.org/0000-0001-6382-3619>

<sup>d</sup>  <https://orcid.org/0000-0003-2827-5092>

superhot geothermal wells. This model is validated by a code-to-code approach, particularly the results provided by the commercial software Eclipse are assumed as benchmark. However, the study resulted almost generic and more relevant results would be provided applying this model to more realistic and detailed cases study. Ref. (Lamy-Chappuis, 2022) in detail models the heat transfer phenomena occurring in a geothermal well. The main assumptions of this model are: i) 1-D approach; ii) constant temperature at an infinite distance from the geothermal well; iii) heat transfer does not occur in the extraction zone and injection zone; iv) constant working fluid velocity; v) the heat exchange occurs only in radial way; vi) the heat exchange along the axis of the pipe is neglected. The simulation model is developed using MATLAB software. This model simulates a desalination plant which exploits the geothermal energy for producing drinkable water. The proposed model resulted extremely sensitive to: i) the geothermal gradient; ii) geothermal well depth and iii) water to be desalinated dissolved solids. The model proved that a geothermal well of a depth of 4000 m, featured by geothermal gradient of  $0.05^{\circ}\text{C}/\text{m}$ , may produce roughly  $600 \text{ m}^3/\text{day}$  of freshwater.

### 1.1 Aim and Novelty

As investigated in the literature review, many works simulate the performances of geothermal wells, comparing with experimental data. Unfortunately, in the framework of geothermal well mathematical modelling, none of the available models is focused on the dynamic response of the well and on the coupling with a detailed geothermal plant. Therefore, the aim and novelty of the present work are:

- Present a model which is suitably detailed but not too computationally heavy to carry out dynamic simulations in complex and detailed geothermal plant layouts.
- Investigate the behavior of the transient model when the operating parameters are varied.
- Evaluate the optimal control strategies for the different operating conditions analyzed, during transient operation.

## 2 MODEL

This work presents the evaluation of the performance of a geothermal well, focusing on the heat exchange phenomena, by means of a thermodynamic model developed in a previous work by some of the authors

of this paper. Note that the focus of this work is on the heat exchange phenomena that occur within the well, which are important for assessing the overall energy performance of the well and the related geothermal plant. In addition, the thermodynamic model will be used to simulate the heat transfer and fluid flow within the well, and to predict the thermal response of the well under different operating conditions. This model simulates a stratified well, including two downhole heat exchangers and ten potential double ports. The double ports are employed for describing the water withdrawn from the well, by means of a submerged pump, which can be located at any well depth. However, in the framework of this research the submerged pumps are located at a selected height (close to the well top). The internal heat exchangers are used with the aim of modelling the downhole heat exchangers installed inside the well. Figure 1 displays the simplified scheme of the geothermal well. In particular, only two heat exchangers and one double port are considered. A double port represents a couple of inlet/outlet to/from the well. The mass balance must be maintained through the double port. This means that the amount of mass flowing into the well through the inlet port must be equal to the amount of mass flowing out of the well through the outlet port. When the geothermal brine is withdrawn from the top of the geothermal well by means of the submerged pump, the geothermal brine simultaneously enters the bottom of the well from the geothermal ground. Thus, the heat continuously enters the well by inlet groundwater openings. The two heat exchangers (Figure 1) are linked for modelling the performance of a downhole heat exchanger inside the geothermal well. The geothermal well is divided in a suitable number of nodes ( $N_{node}$ ). Each node represents a layer of the stratified well as a function of the vertical gradient of the temperature. In each layer the volume is assumed fully mixed. The energy balance is performed for each layer of the well to perform a detailed calculation of each node's temperature. Obviously, this approach leads to a discrete temperature stratification. The nodes temperatures are evaluated by solving a set of differential equations. The data necessary for describing the well thermodynamic performance are stored in a  $N_{node} \times 3$  array. The first column ( $j=1$ ) consists of the data about the first heat exchanger, the second one ( $j=2$ ) includes the data of the well, and the last column ( $j=3$ ) consists of the data of the second heat exchanger. The energy balance of each well ( $j=2$ ) node ( $i$ ) is displayed in the following equation:

$$\begin{aligned}
 \frac{V_w \cdot \rho_w \cdot c_{p,w}}{N_{\text{node}}} \cdot \frac{\partial t_{i,2}}{\partial \vartheta} = & \sum_{p=1}^{10} \dot{m}_{dp} \cdot c_{p,w} \cdot \left[ \xi_1 \cdot (t_{i-1,2} - t_{i,2}) + \xi_2 \cdot (t_{i,2} - t_{i+1,2}) \right] + \\
 & \xi_3 \cdot \frac{(UA)_{h1,w}^*}{n_{h1}} \cdot (t_{i,1} - t_{i,2}) + \xi_4 \cdot \frac{(UA)_{h2,w}^*}{n_{h2}} \cdot (t_{i,3} - t_{i,2}) + \\
 & \lambda_{\text{con}} \cdot \frac{A_q}{H_w} \cdot N_{\text{node}} \cdot \left[ (t_{i+1,2} - t_{i,2}) + (t_{i-1,2} - t_{i,2}) \right] - \frac{(UA)_{w,wk}}{n \cdot dzk} \cdot (t_{i,2} - t_{ww})
 \end{aligned} \quad (1)$$

where:  $n_{h1}$  is the number of nodes occupied by the heat exchangers 1;  $U$  is the overall heat transfer coefficient;  $A$  is the exchange area;  $n_{h2}$  is the number of nodes occupied by the heat exchangers 2;  $\lambda_{\text{con}}$  is the effective thermal conductivity in the well.

A mass flow from the top to the bottom counts negative, and vice versa positive, the logical variables,  $\xi_i$  are evaluated as follows:

- $\xi_1 = 0$  if  $\dot{m}_{dp} < 0$ , else  $\xi_1 = 1$ ;
- $\xi_2 = 0$  if  $\dot{m}_{dp} > 0$ , else  $\xi_2 = 1$ ;
- $\xi_3 = 0$  if the store node  $i$  is not in contact with the node  $i$  of heat exchanger 1, else  $\xi_3 = 1$ ;

- $\xi_4 = 0$  if the store node  $i$  not is in contact with the node  $i$  of heat exchanger 2, else  $\xi_4 = 1$ .

The first term of equation 1 described the internal energy variation of each node as function of the time. Considering the right-hand side of the equation, the first sum describes the heat transfer due to the mass flows throughout the nodes. The second and third term describe the heat transfer between well node and heat exchanger node. The fourth represents the thermal conduction between the layers in the well. The last term describes the heat losses to the well surroundings, i.e. the rock of the groundwater. The energy balance of heat exchanger nodes is described by the following equation:

$$\begin{aligned}
 \frac{V_{hy} \cdot \rho_{hy} \cdot c_{p,hy}}{n_{hy}} \cdot \frac{\partial t_{i,j}}{\partial \vartheta} = & \xi_5 \cdot \dot{m}_{hy} \cdot c_{p,hy} \cdot (t_{i-1,j} - t_{i,j}) + \xi_6 \cdot \dot{m}_{hy} \cdot c_{p,hy} \cdot (t_{i,j} - t_{i+1,j}) + \\
 & \frac{(UA)_{hy,w}^*}{n_{hy}} \cdot (t_{i,2} - t_{i,j}) - \frac{(UA)_{hy,ww}}{n_{hy}} \cdot (t_{i,j} - t_{ww})
 \end{aligned} \quad (2)$$

where  $t_{i\pm 1,j}$  represents the inlet ( $i+1$ ) and outlet ( $i-1$ ) temperature of the heat exchanger. In particular:

- $\xi_5 = 1$  if  $\dot{m}_{hy} > 0$ , else  $\xi_5 = 0$ ;
- $\xi_6 = 1$  if  $\dot{m}_{hy} < 0$ , else  $\xi_6 = 0$ .

Note that  $(UA)_{hy,ww}$ , which describes the heat loss capacity rate from the heat exchangers to surroundings, is assumed equal to zero. The heat

exchangers are totally immersed into the geothermal brine.

Obviously, this model dynamically describes the energy performance of the geothermal well and of the considered heat exchangers. The temperature of the well is selected according to experimental measurements carried out by INGV (Kiaghadi, 2017) (Italian National Institute of geology and volcanology). The main simulation assumptions are displayed in Table 1.

Table 1: Geothermal well data and simulation assumptions.

	Definition	Value	Unit
$T_{\text{well}}$	Temperature of the well	96 ( <a href="http://terremoti.ingv.it/contact2018">http://terremoti.ingv.it/contact2018</a> )	°C
$m_{HE}$	Mass flow rate of HE	500	kg/h
$m_{\text{brine}}$	Brine mass flow rate	0	kg/h
$H_w$	Height of the well	69	m
$N_{\text{node}}$	Number of nodes	150	-

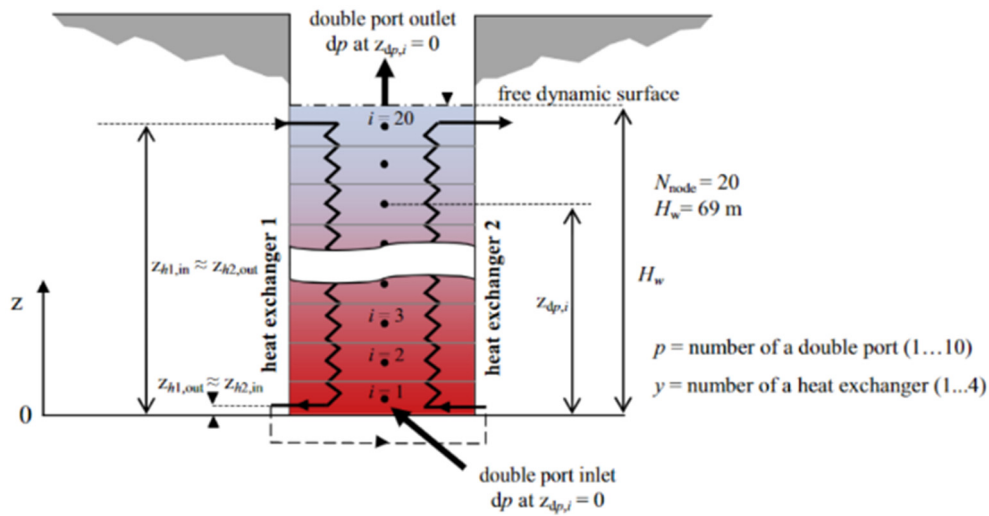


Figure 1: Scheme of the proposed model of the geothermal well.

### 3 RESULTS

The processor Interl(R) Core(TM) i7-7700 with a ram of 8 GB is used for carrying out the simulations. Adopting a time step of 0.01 h, and a time horizon of 100 hours a simulation time of 180 s is detected. Figure 2 displays the outlet temperature of the downhole heat exchanger ( $T_{HEout}$ ) as a function of the time, for two different user thermal load, i.e.,  $P_{th,user} = 5 \text{ kW}_{th}$  and  $P_{th,user} = 8 \text{ kW}_{th}$ . With a withdrawn thermal flow rate of  $5 \text{ kW}_{th}$ , the temperature decreases from the initial value of  $95.90 \text{ }^\circ\text{C}$  to  $91.98 \text{ }^\circ\text{C}$ , reaching the steady state. Note that the steady state is reached in about 25 hours for both the analyzed cases (Figure 2). These results show that the model can mimic the dynamic evolution of a geothermal well in operation. Note that the selected submerged pump is supposed to be switched off (Table 1).

Figure 3 shows dynamic response of the geothermal well under several different operative conditions, i.e., different user thermal loads ( $P_{HEout}$ ), without activating the submerged pump. Obviously, the greater the withdrawing of thermal flow rate, the lower the outlet temperature of HE ( $T_{HEout}$ ). In particular, with a withdrawn thermal flow rate of  $15 \text{ kW}_{th}$ , the HE outlet temperature falls below  $85 \text{ }^\circ\text{C}$  in about 8 hours. Thus, the proposed model is quite responsive to the thermal load. This feature could be useful for predicting whether a thermal load would dramatically reduce the well temperature beyond an assumed threshold temperature. It is worth nothing that the selected geothermal well is mainly heated by the hot groundwater. In fact, the rocks surrounding

the geothermal well have a hot temperature, i.e., roughly  $90\text{--}96\text{ }^\circ\text{C}$ , but the convective and conductive heat transfer phenomena are not able to balance high heat transfer rate loads. Conversely, the withdrawal of geothermal brine makes the hotter brine located beyond the geothermal well enter the geothermal well, heating it up. Therefore, to increase the available heat, without reducing the heat exchanger outgoing temperature, a suitable amount of geothermal brine should be withdrawn. In this framework, a parametric analysis is carried out to analyze the combined effect of brine flow rate and downhole heat exchanger thermal load on the geothermal well performance (Figure 4). The growth of the brine mass flow rate ( $m_{brine}$ ) increases the thermal energy charged in the geothermal well, increasing the thermal capacity of the geothermal well. In fact, as discussed before, the increase in the brine flow rate makes higher amount of hot water ( $T_{brine} = 97\text{ }^\circ\text{C}$ ) to enter the well. Thus, the well can match extremely high thermal load without a significant reduction of the heat exchanger outlet temperature. For example,  $T_{HEout}$  is equal to  $90\text{ }^\circ\text{C}$  with a withdrawn thermal flow rate of  $50 \text{ kW}_{th}$  and a  $m_{brine}$  of  $4100 \text{ kg/h}$ , (Figure 4). In addition, this figure may be useful for dimensioning the geothermal well plant. To match a thermal load of  $21 \text{ kW}_{th}$ , without reducing the heat exchanger temperature below  $90\text{ }^\circ\text{C}$ , the submerged pump should withdraw a brine flow rate ( $m_{brine}$ ) greater than  $2100 \text{ kg/h}$ .

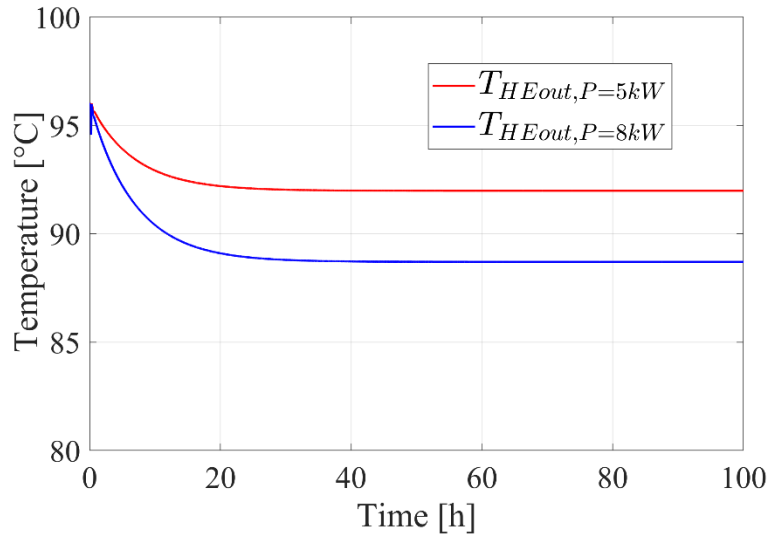


Figure 2: Geothermal well model dynamic thermal performance.

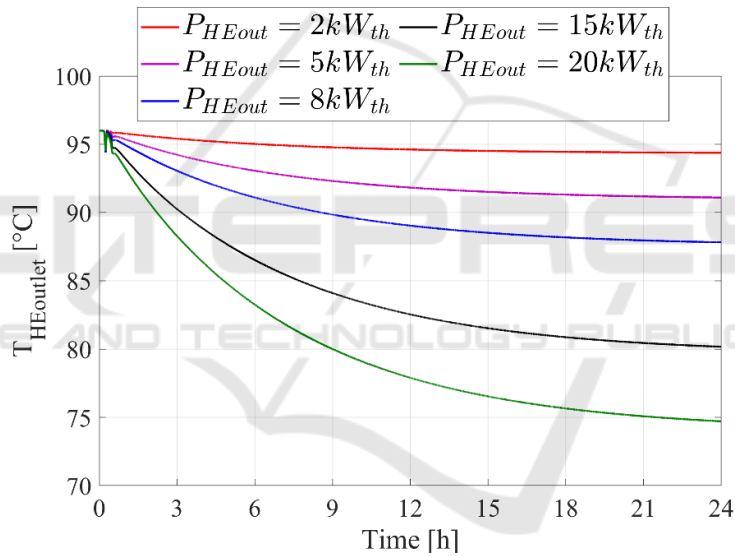


Figure 3: Well discharging as function of different operative conditions.

In addition, this model provides useful guidelines for the development of proper control strategies to ensure the correct operating conditions of the geothermal well. Figure 5 displays the dynamic response of the geothermal well under two different control strategies: C1 proportional control strategy and C2 on off control strategy. In particular, control strategies C1 and C2 are designed for keeping the heat exchanger outlet temperature within the range 85-90°C. Then, the controlled variable is the temperature of the water leaving the downhole heat exchanger, while the control signal of the controller manages the submerged pump, withdrawing geothermal brine from the geothermal well. Note that a constant

thermal load of 10 kW<sub>th</sub> is withdrawn from the download heat exchanger and the rated mass flow rate of the submerged pump is equal to 2100 kg/h. According to C1,  $m_{brine}$  resulted equal to 1152 kg/h, with a  $T_{HEout}$  equal to 87.3°C. Therefore, the controller achieves the goal of keeping the downhole heat exchanger outlet temperature within the assumed range. Regarding control strategy C2, when the  $T_{HEout}$  decreases to 85°C the submerged pump is activated, withdrawing the rated brine flow rate, equal to 2100 kg/h. This allows the surrounding water, which is at a higher temperature level, to enter the well and increase its temperature. Then, when the  $T_{HEout}$  reaches the selected upper bound (95°C), the pump is

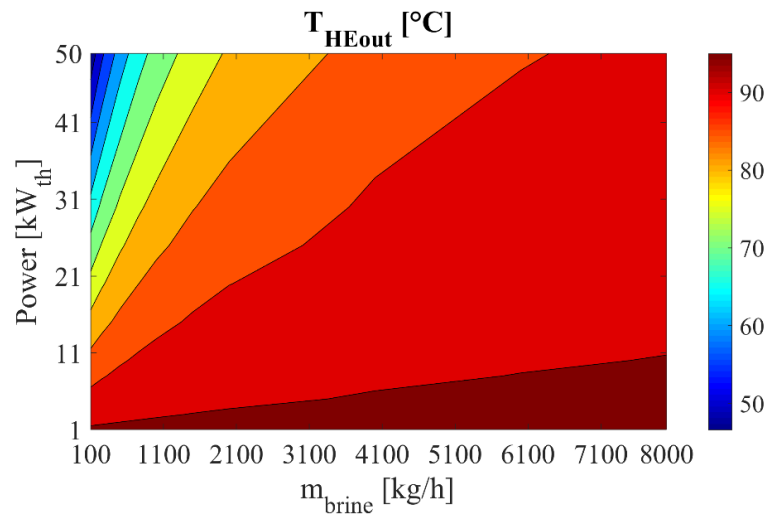


Figure 4: Parametrical analysis changing both brine mass flow rate and heat exchanger withdrawn power.

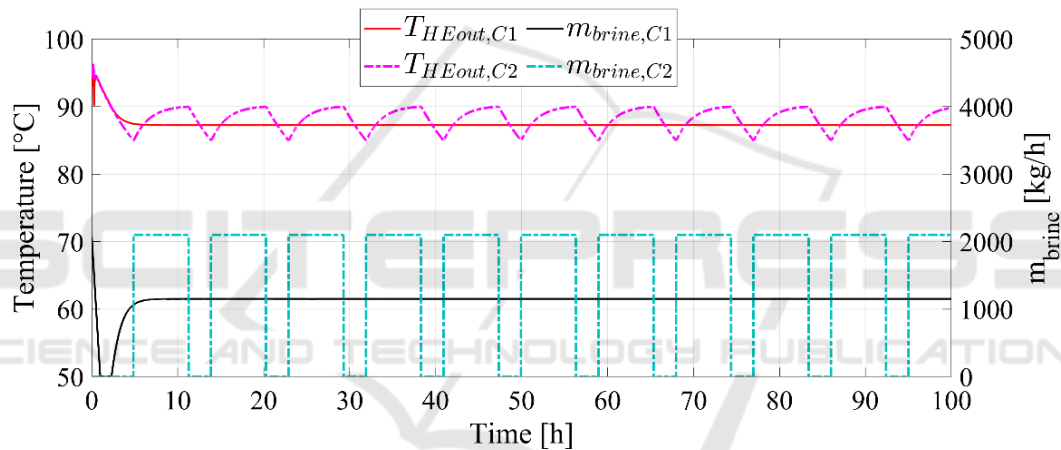


Figure 5: Downhole heat exchanger outlet water temperature, under two different geothermal well control strategy, namely C1 dead band on-off controller and C2 proportional controller.

switched off. Figure 6 displays the response of the proportional controller when the thermal energy demand of the user fluctuates. In particular, two different forcing functions are selected for testing the geothermal well model and the controller. The first one consists of a sinusoidal thermal energy demand with an amplitude of 1 kW and a period of 14 hours, the second one consists of a sinusoidal thermal energy demand with an amplitude of 5 kW and a period of 20 hours. This figure proves the stability and reliability of the proposed model and of the controller. In fact, the controller can keep the temperature within the selected range, i.e., 85-90°C. In particular, the controller follows the fluctuating thermal energy demand properly modulating the brine flow rate, leading to very slight oscillation of the temperature. In fact,  $T_{HEout}$  varies between 86.9-87.4°C for the first

forcing function, while  $T_{HEout}$  varies between 88-86.4°C for the second forcing function. In conclusion, thanks to the great accuracy and sensibility of the proposed model, this could be also adopted for developing proper control strategies to manage geothermal well dynamic operations.

## 4 CONCLUSIONS

This work deals with a numerical model of a geothermal well, allowing one to dynamically simulate the energy performance of the well and the related downhole heat exchangers. The model of the geothermal well is developed in TRNSYS environment. In addition, this model is designed for being reliable and computationally fast, to integrate

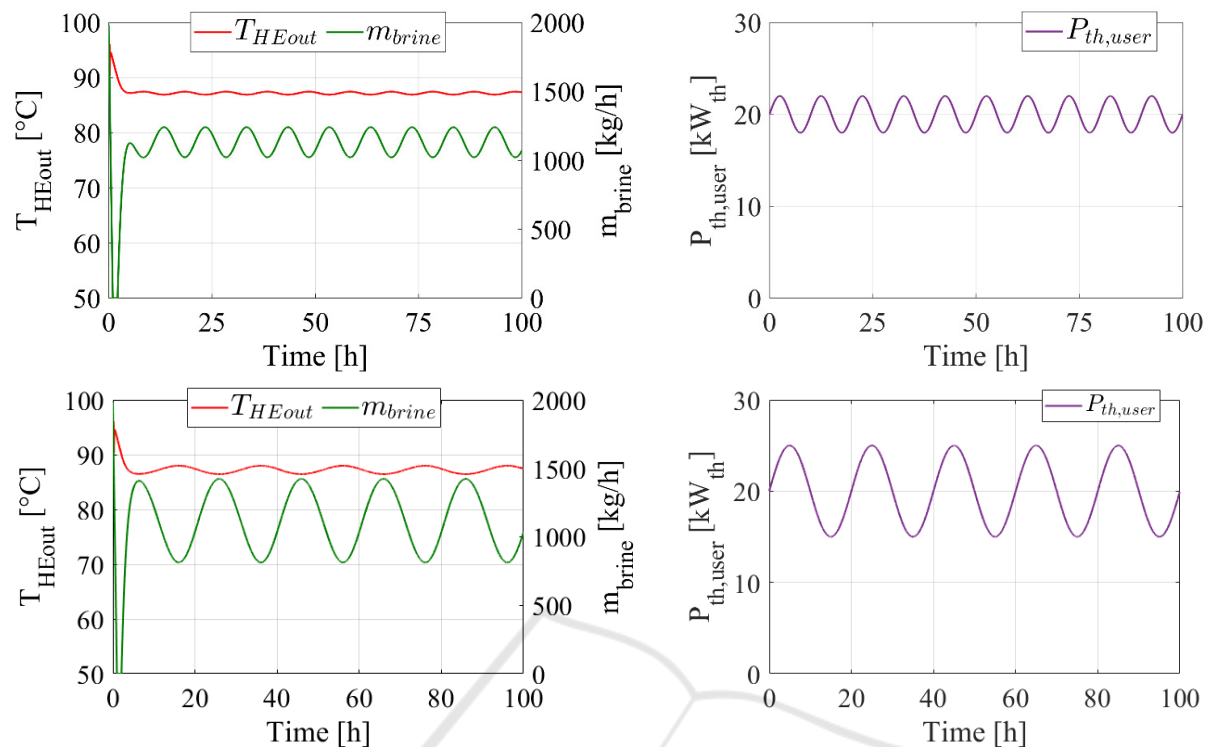


Figure 6: Heat exchanger outlet temperature controlled by means of proportional controller, under two different user thermal energy demands.

such model in more detailed dynamic model of geothermal power plants. The results show that the model can mimic the dynamical performance of the well under several operative condition and control strategies. In particular, the model resulted extremely responsive to the user thermal load and to the withdrawn brine.

## REFERENCES

- Buonomano, A., F. Calise, A. Palombo and M. Vicidomini (2015). "Energy and economic analysis of geothermal-solar trigeneration systems: A case study for a hotel building in Ischia." *Applied Energy* 138: 224-241.
- Calise, F., F. L. Cappiello, M. Dentice d'Accadia, F. Petrakopoulou and M. Vicidomini (2022). "A solar-driven 5th generation district heating and cooling network with ground-source heat pumps: a thermo-economic analysis." *Sustainable Cities and Society* 76: 103438.
- Calise, F., F. L. Cappiello, M. Dentice d'Accadia and M. Vicidomini (2020). "Thermo-Economic Analysis of Hybrid Solar-Geothermal Polygeneration Plants in Different Configurations." 13(9): 2391.
- Dalala, Z., M. Al-Omari, M. Al-Addous, M. Bdour, Y. Al-Khasawneh and M. Alkasrawi (2022). "Increased renewable energy penetration in national electrical grids constraints and solutions." *Energy* 246: 123361.
- Glassley, W. E. (2014). *Geothermal energy: renewable energy and the environment*, CRC press.
- <http://terremoti.ingv.it/contact>. (2018). "<http://terremoti.ingv.it/contact>." from <http://terremoti.ingv.it/contact>.
- Kiaghadi, A., R. S. Sobel, and H. S. Rifai (2017). "Modeling geothermal energy efficiency from abandoned oil and gas wells to desalinate produced water." *Desalination* 414: 51-62.
- Lamy-Chappuis, B., A. Yapparova and T. Driesner (2022). "Advanced well model for superhot and saline geothermal reservoirs." *Geothermics* 105: 102529.
- McClellan, A., and O. W. Pedersen (2023). "The role of regulation in geothermal energy in the UK." *Energy Policy* 173: 113378.
- Stefánsson, V. (2002). "Investment cost for geothermal power plants." *Geothermics* 31(2): 263-272.
- Tapia, C., B. Abajo, E. Feliu, M. Mendizabal, J. A. Martinez, J. G. Fernández, T. Laburu and A. Lejarazu (2017). "Profiling urban vulnerabilities to climate change: An indicator-based vulnerability assessment for European cities." *Ecological Indicators* 78: 142-155.
- Yuan, W., Z. Chen, S. E. Grasby, E. Little and G. Zhao (2023). "Thermodynamic Modeling of the Advanced Geothermal System Using Inclined Well Applications." *Applied Thermal Engineering* 220: 119709.
- Yuan, W., Z. Chen, S. E. Grasby, E. Little and G. Zhao (2023). "Thermodynamic Modeling of the Advanced Geothermal System Using Inclined Well Applications." *Applied Thermal Engineering* 220: 119709.